Nonequilibrium Fluctuations and Mechanochemical Couplings of a Molecular Motor

A. W. C. Lau,[1] D. Lacoste,[2] and K. Mallick[3]

[1]*Department of Physics, Florida Atlantic University, 777 Glade Rd., Boca Raton, Florida 33431, USA*
[2]*Laboratoire de Physico-Chimie Théorique, UMR 7083, ESPCI, 10 rue Vauquelin, 75231 Paris Cedex 05, France*
[3]*Service de Physique Théorique, CEA Saclay, 91191 Gif, France*

(Received 3 March 2007; published 8 October 2007)

We investigate theoretically the violations of Einstein and Onsager relations and the thermodynamic efficiency for a single processive motor operating far from equilibrium using an extension of the two-state model introduced by Kafri *et al.* [Biophys. J. **86**, 3373 (2004)]. With the aid of the Fluctuation Theorem, we analyze the general features of these violations and this efficiency and link them to mechanochemical couplings of motors. In particular, an analysis of the experimental data of kinesin using our framework leads to interesting predictions that may serve as a guide for future experiments.

DOI: 10.1103/PhysRevLett.99.158102 PACS numbers: 87.16.Nn, 05.40.−a, 05.70.Ln

Motor proteins are nanomachines that convert chemical energy into mechanical work and motion [1]. Important examples include kinesin, myosin, and RNA polymerase. Despite a number of theoretical models [2–6], understanding the mechanochemical transduction mechanisms behind these motors remains a significant challenge [7]. Recent advances in experimental techniques [8,9] to probe the fluctuations of single motors provide ways to gain insight into their kinetic pathways [10]. However, a general description for fluctuations of systems driven out of equilibrium, and, in particular, of motors, is still lacking. Recently, the Fluctuation Theorem (FT) [11–13] has emerged as a promising framework to characterize fluctuations in far-from-equilibrium regimes where Einstein and Onsager relations no longer hold [12]. In a nutshell, FT states that the probability distribution for the entropy production rate obeys a symmetry relation, and it has been verified in a number of beautiful experiments on biopolymers and colloidal systems [14]. In this Letter, we demonstrate that FT provides a natural framework in which thermodynamic constraints can be imposed on the operation of nanomachines far from equilibrium.

Specifically, we study a generalization of the two-state model of motors introduced in Ref. [5]. Although similar models have been investigated with known exact results [4,5], we reformulate the model to include an important variable, namely, the number of adenosine triphosphate (ATP) consumed, and construct a thermodynamic framework. Our framework allows us to characterize the ATP consumption rate of a motor, its run length, and its thermodynamic efficiency. Additionally, we show that our model obeys FT [13]. While there have been a few recent studies proving FT for motors [15–17], we further investigate the physical implications of FT here. In particular, we quantify the violations of Einstein and Onsager relations, respectively, by four temperaturelike parameters, T_{ij}, and by the difference of the mechanochemical coupling coefficients, $\Delta\lambda$, and we explore the behaviors of T_{ij} and $\Delta\lambda$, as well as the motor efficiency, as functions of generalized forces with the aid of FT. Our main results are (i) one of the Einstein relations holds near stalling, (ii) the degree by which the Onsager symmetry is broken ($\Delta\lambda \neq 0$) is largely determined by the underlying asymmetry of the substrate, (iii) only two "effective" temperatures characterize the fluctuations of tightly coupled motors, and (iv) kinesin's maximum efficiency and its maximum violation of Onsager symmetry occur roughly at the same energy scale, corresponding to that of an ATP hydrolysis ($\sim 20 k_B T$).

As a result of conformational changes powered by hydrolysis of ATP, a linear processive motor, like kinesin, moves along a one-dimensional substrate (microtubules). Its state may be characterized by two variables: its position and the number of ATP consumed. To model its dynamics, we consider a linear discrete lattice, where the motor "hops" from one site to neighboring sites, either consuming or producing ATP (see Fig. 1). The position is denoted by $x = nd$, where $2d \approx 8$ nm is the step size for kinesin. The even sites (denoted by a) are the low-energy state of the motor, whereas the odd sites (denoted by b) are its high-energy state; their energy difference is $\Delta E \equiv k_B T \epsilon$,

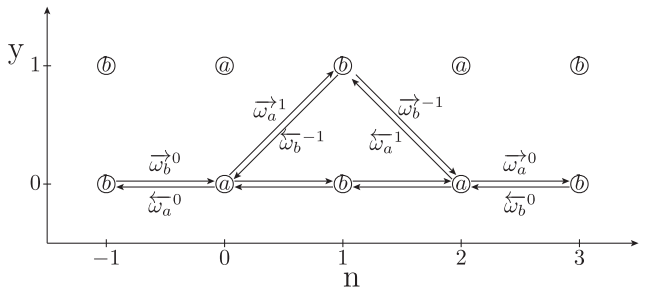

FIG. 1. A schematic of the rates of the two-state model for a molecular motor moving on a linear lattice with y number of ATP consumed. The even and odd sites are denoted by a and b, respectively. In the case of two-headed kinesin, site a represents a state where both heads are bound to the filament, whereas site b represents a state with only one head bound.

where k_B is the Boltzmann constant and T is the temperature.

Because of the periodicity of the filament, all the even (a) sites and all the odd (b) sites are equivalent. The dynamics are governed by a master equation for the probability, $P_i(n, y, t)$, that the motor, at time t, has consumed y units of ATP and is at site i ($=a, b$) with position n:

$$\partial_t P_i(n, y, t) = -(\overleftarrow{\omega}_i + \overrightarrow{\omega}_i)P_i(n, y, t) + \sum_{l=-1,0,1} [\overleftarrow{\omega}_j^l P_j(n+1, y-l, t) + \overrightarrow{\omega}_j^l P_j(n-1, y-l, t)], \quad (1)$$

with $i \neq j$, where $\overleftarrow{\omega}_j \equiv \sum_l \overleftarrow{\omega}_j^l$ and $\overrightarrow{\omega}_j \equiv \sum_l \overrightarrow{\omega}_j^l$. Denoted by $\overleftarrow{\omega}_j^l$ and $\overrightarrow{\omega}_j^l$ are the transition probability per unit time for the motor, with $l(=-1, 0, 1)$ ATP molecules consumed, to jump from site j to a neighboring site to the left or to the right, respectively.

The transition rates can be constructed by considering the kinetics of the transitions between the two states M_a and M_b of the motor [3]. We assume two different chemical pathways: (α) $M_a + \mathrm{ATP} \rightleftharpoons M_b + \mathrm{ADP} + P$, ($\beta$) $M_a \rightleftharpoons M_b$. The α pathway represents the transition of the motor accompanied by ATP hydrolysis, and the β pathway represents the transition driven by thermal activation. It is straightforward to generalize the model with more chemical pathways, but here we focus only on these two, for which $\overleftarrow{\omega}_b^1 = \overrightarrow{\omega}_a^{-1} = \overleftarrow{\omega}_a^{-1} = \overrightarrow{\omega}_b^1 = 0$. Following Ref. [4], the transition rates in the presence of an external force F_e are changed according to $\overleftarrow{\omega}_i^l(F_e) = \overleftarrow{\omega}_i^l(0)e^{-\theta_i^- f}$ and $\overrightarrow{\omega}_i^l(F_e) = \overrightarrow{\omega}_i^l(0)e^{+\theta_i^+ f}$, where $f \equiv F_e d/(k_B T)$ and $\theta_i^\pm$ are the load distribution factors [4]. These load distribution factors take into account that the external force may not distribute uniformly among different transitions. After one period, the work done by F_e on the motor is $-F_e 2d$, implying that $\theta_a^+ + \theta_b^- + \theta_a^- + \theta_b^+ = 2$ [4]. Thus, we may write the nonzero rates as

$$\begin{aligned} \overleftarrow{\omega}_b^{-1} &= \alpha e^{-\theta_b^- f}, & \overleftarrow{\omega}_b^{0} &= \omega e^{-\theta_b^- f}, \\ \overrightarrow{\omega}_a^{1} &= \alpha e^{-\epsilon+\Delta\mu+\theta_a^+ f}, & \overrightarrow{\omega}_a^{0} &= \omega e^{-\epsilon+\theta_a^+ f}, \\ \overleftarrow{\omega}_a^{1} &= \alpha' e^{-\epsilon+\Delta\mu-\theta_a^- f}, & \overleftarrow{\omega}_a^{0} &= \omega' e^{-\epsilon-\theta_a^- f}, \\ \overrightarrow{\omega}_b^{-1} &= \alpha' e^{\theta_b^+ f}, & \overrightarrow{\omega}_b^{0} &= \omega' e^{\theta_b^+ f}, \end{aligned} \quad (2)$$

where α and α' and ω and ω' are the bare rates for the two distinct transitions for the pathways and $\Delta\tilde{\mu} \equiv k_B T \Delta\mu$ is the chemical potential difference [3]. The underlying asymmetry of the substrate dictates that $\alpha \neq \alpha'$ and $\omega \neq \omega'$ as required for directional motion [5].

We find that the rates in Eq. (2) satisfy four generalized detailed balance conditions:

$$\overrightarrow{\omega}_b^{-l} P_b^{\mathrm{eq}} = \overleftarrow{\omega}_a^{l} P_a^{\mathrm{eq}} e^{+(\theta_a^- + \theta_b^+)f - \Delta\mu l}, \quad (3)$$

$$\overleftarrow{\omega}_b^{-l} P_b^{\mathrm{eq}} = \overrightarrow{\omega}_a^{l} P_a^{\mathrm{eq}} e^{-(\theta_a^+ + \theta_b^-)f - \Delta\mu l}, \quad (4)$$

for $l = 0, 1$, where $P_a^{\mathrm{eq}} = 1/(1+e^{-\epsilon})$ and $P_b^{\mathrm{eq}} = e^{-\epsilon}/(1+e^{-\epsilon})$ are the equilibrium probabilities corresponding to $f = 0$ and $\Delta\mu = 0$. We note that these relations, Eqs. (3) and (4), while valid arbitrary far from equilibrium, still refer to the equilibrium state via the probabilities P_i^{eq}. We show below that these relations lead to a FT [13]. Introducing the generating functions, $F_i(z_1, z_2, t) \equiv \sum_y \sum_n e^{-z_1 n - z_2 y} P_i(n, y, t)$, whose time evolution is governed by $\partial_t F_i = \mathcal{M}_{ij} F_j$, where $\mathcal{M}[z_1, z_2]$ is a 2×2 matrix that can be obtained from Eq. (1), we find $\langle e^{-z_1 n - z_2 y} \rangle = \sum_i F_i(z_1, z_2, t) \sim \exp(\vartheta t)$, for $t \to \infty$, where $\vartheta \equiv \vartheta[z_1, z_2]$ is the largest eigenvalue of $\mathcal{M}$. Using Eqs. (3) and (4), it can be shown that $\mathcal{M}$ and $\mathcal{M}^\dagger$ are related by a similarity transformation: $\mathcal{M}^\dagger[f - z_1, \Delta\mu - z_2] = \mathcal{Q}\mathcal{M}[z_1, z_2]\mathcal{Q}^{-1}$, where $\mathcal{M}^\dagger$ is the adjoint of $\mathcal{M}$ and $\mathcal{Q}$ is a diagonal matrix. This similarity relation implies that

$$\vartheta[z_1, z_2] = \vartheta[f - z_1, \Delta\mu - z_2], \quad (5)$$

which is one form of FT.

Now, we proceed to discuss the physical consequences of FT. The eigenvalue, ϑ, contains all the steady-state properties of the motor. In particular, the average (normalized) velocity, $\hat{v} = v/d$, and the average ATP consumption rate, r, are, by definition, given by $\hat{v} = -\partial_{z_1}\vartheta[0, 0]$ and $r = -\partial_{z_2}\vartheta[0, 0]$, respectively [18]. From the conditions $\hat{v} = 0$ and $r = 0$, we can construct a full operation diagram of a motor, as shown in Fig. 2 for the case of kinesin. The

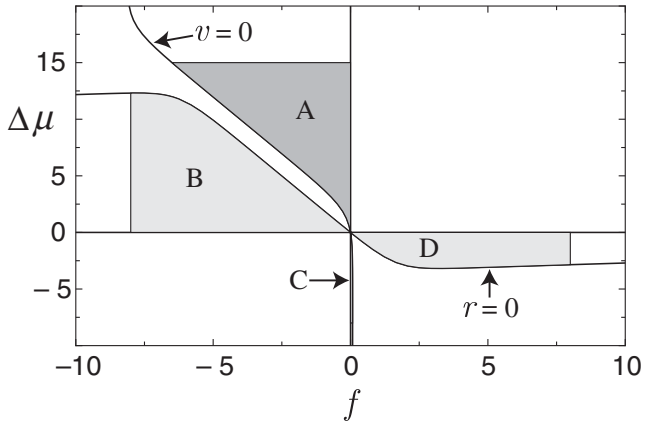

FIG. 2. Four modes of operation of a molecular motor, as delimited by $\hat{v} = 0$ and $r = 0$ [2]. The lines are generated with parameters that we have extracted from fitting the data for kinesin in Ref. [8] to our model. (The best-fit values for the parameters are listed at the end of the text.) In Region A, where $r\Delta\mu > 0$ and $f\hat{v} < 0$, the motor uses chemical energy of ATP to perform mechanical work. In Region B, where $r\Delta\mu < 0$ and $f\hat{v} > 0$, the motor produces ATP from mechanical work. In Region C, where $r\Delta\mu > 0$ and $f\hat{v} < 0$, the motor uses adenosine diphosphate to perform mechanical work. In Region D, where $r\Delta\mu < 0$ and $f\hat{v} > 0$, the motor produces adenosine diphosphate from mechanical work.

curves $\hat{v} = 0$ and $r = 0$ define implicitly $f = f_{st}(\Delta\mu)$ (the stalling force) and $\Delta\mu = \Delta\mu_{st}(f)$, respectively. It is interesting to note that the large asymmetry between regions A and C in Fig. 2 reflects the fact that kinesin is a unidirectional motor.

The response and fluctuations of a motor are quantified, respectively, by a response matrix λ_{ij} and by a diffusion matrix $2D_{ij} = \partial z_i \partial z_j \vartheta[0, 0]$. The physical meanings of λ_{ij} are: $\lambda_{11} \equiv \partial\hat{v}/\partial f$ is the mobility, $\lambda_{22} \equiv \partial r/\partial\Delta\mu$ is the chemical admittance, and more importantly, $\lambda_{12} \equiv \partial\hat{v}/\partial\Delta\mu$ and $\lambda_{21} \equiv \partial r/\partial f$ are the Onsager coefficients that quantify the mechanochemical couplings of the motor. Differentiating Eq. (5), we can write

$$\begin{aligned} \hat{v} &\equiv -\partial_{z_1}\vartheta[0, 0] = \partial_{z_1}\vartheta[f, \Delta\mu], \\ r &\equiv -\partial_{z_2}\vartheta[0, 0] = \partial_{z_2}\vartheta[f, \mu]. \end{aligned} \tag{6}$$

Near equilibrium, where f and $\Delta\mu$ are small, a Taylor expansion of Eq. (6) leads to $\hat{v} = \lambda^0_{11} f + \lambda^0_{12}\Delta\mu$ and $r = \lambda^0_{21} f + \lambda^0_{22}\Delta\mu$, with $\lambda^0_{ij} = \partial_{z_i}\partial_{z_j}\vartheta[0, 0] \equiv D_{ij}$, which are the Einstein relations, and $\lambda^0_{12} \equiv \partial_{z_2}\partial_{z_1}\vartheta[0, 0] = \partial_{z_1}\partial_{z_2}\vartheta[0, 0] \equiv \lambda^0_{21}$, which is the Onsager relation. Thus, FT captures the response and fluctuations near equilibrium [12,17].

Away from equilibrium, we expect that Onsager and Einstein relations are no longer valid. To quantify their violations, we introduce $\Delta\lambda \equiv \lambda_{12} - \lambda_{21}$ and four ''temperature''-like quantities, $T_{ij} \equiv D_{ij}/\lambda_{ij}$. Of course, these effective temperatures are not thermodynamic temperatures: they are merely one of the ways to quantify deviations of Einstein relations. Via FT, we obtain the following general characterizations for these quantities. First, at sufficiently small driving, we find $2\Delta\lambda \approx (\partial_{\Delta\mu}\vartheta_{11} - \partial_f\vartheta_{12})f + (\partial_{\Delta\mu}\vartheta_{12} - \partial_f\vartheta_{22})\Delta\mu$, where $\vartheta_{ij} \equiv \partial z_i \partial z_j \vartheta[f/2, \Delta\mu/2]$. In particular, for $f \ll 1$, $\Delta\lambda \propto \Delta\mu$. Thus, active processes in the mechanochemical transduction mechanism break Onsager symmetry and these processes can be studied via $\Delta\lambda$. Secondly, along $\hat{v}(f, \Delta\mu) = 0$, we find that Eq. (4) has a special relation: $\vartheta[z_1, 0] = \vartheta[\delta f - z_1, 0]$, where $\delta f = f - f_{st}(\Delta\mu)$. Therefore, one of the Einstein relations, $\lambda_{11} = D_{11}$, holds near stalling, since FT implies that $2\hat{v} = \partial^2_{z_1}\vartheta[0, 0]\delta f$ for small δf. Note that this particular Einstein relation also holds for ratchet models under similar conditions [19]. By the same token, near $r = 0$, FT implies that an Einstein relation holds for y, i.e., $D_{22} = \lambda_{22}$.

For our two-state model, we can fully investigate the behaviors of $\Delta\lambda$ and T_{ij}. Let us focus on Region A of Fig. 2 and $-f \ll 1$, so that λ_{ij} and T_{ij} depend only on $\Delta\mu$. In Fig. 3(a), we display $\Delta\lambda$ and the three distinct T_{ij} (see below) as a function of $\Delta\mu$. We observe that for small $\Delta\mu$, $\Delta\lambda$ rises linearly with $\Delta\mu$, in agreement with the FT prediction, and that for larger $\Delta\mu$, $\Delta\lambda$ exhibits a maximum. Moreover, for large $\Delta\mu$, we find that $\Delta\lambda$ approaches to a constant value. The latter observation can be understood from a simple argument. When $\Delta\mu \gg 1$, the transitions between the states a and b of the motor are limited by the β pathways. Therefore, we can write $r \simeq \omega e^{-\theta_b^- f} + \omega' e^{\theta_b^+ f}$, which implies that for small f, $\Delta\lambda \simeq \omega\theta_b^- - \omega'\theta_b^+$, since $\lambda_{12} \approx 0$ for large $\Delta\mu$. Thus, the underlying asymmetry of the substrate determines the degree by which the Onsager symmetry is broken.

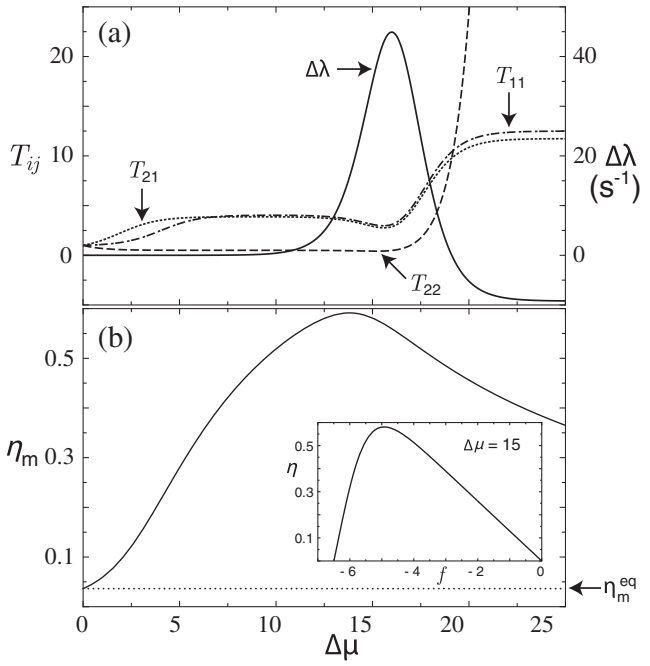

FIG. 3. (a) Plots of T_{11} (dot-dashed), T_{21} (dotted), T_{22} (dashed), and $\Delta\lambda$ (solid) vs $\Delta\mu$ in Region A of Fig. 2 with small f. T_{ij} characterize the fluctuation-response ratios (see text), and $\Delta\lambda$ quantifies the breaking of Onsager symmetry. (b) Local maximum of the efficiency η_m vs $\Delta\mu$. Note that η_m is substantially larger than η_m^{eq} (the dotted line). Note also that the absolute maximum, which occurs at about $\Delta\mu \approx 15$, roughly corresponds also to the maximum of $\Delta\lambda$. Inset: Efficiency vs normalized force for $\Delta\mu = 15$. The parameters used in both (a) and (b) are the same as those used to generate Fig. 2.

In Region A and $-f \ll 1$, the T_{ij} also exhibit interesting behaviors. First, we note that the run length ℓ—the distance moved per ATP hydrolyzed—is independent of $\Delta\mu$: $\ell \equiv v/r = 2d(\alpha\omega' - \alpha'\omega)/[(\alpha + \alpha')(\omega + \omega')] < 2d$. With the help of FT, we find that $T_{12} = T_{22}$ for any $\Delta\mu$. Therefore, there are only three effective temperatures instead of four, as one might naturally suppose. As shown in Fig. 3(a), we observe that all distinct T_{ij} start off at $T_{ij} = 1$ near equilibrium, as expected, and for large $\Delta\mu$, $T_{22} \sim e^{\Delta\mu}$ diverges exponentially, whereas T_{21} and T_{11} approach finite values. Secondly, for tightly coupled motors, $\ell/(2d) \sim 1$, we find that T_{11} is nearly identical to T_{21} [see Fig. 3(a)]. Therefore, in this case, only two effective temperatures characterize motors' fluctuations.

In addition, our framework allows us to investigate the thermodynamic efficiency, an important quantity that also characterizes the working of a motor [20]. In Region A, it is defined as the ratio of the work performed to the chemical

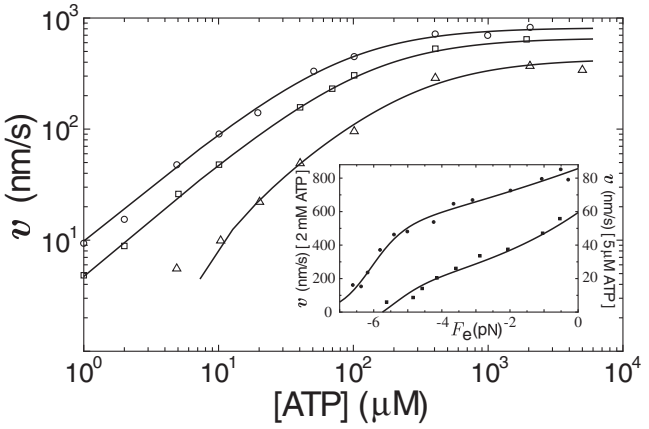

FIG. 4. Kinesin velocity vs ATP concentration under an external force. The solid curves are the fits of our model to data from Ref. [8]. From the top down, the plots are for $F_e = -1.05$, -3.59, and -5.63 pN, respectively. Inset: Kinesin velocity vs force under a fixed ATP concentration. The solid curves are fits to the data of Ref. [8]. From the top down, the plots are for [ATP] = 2 mM and 5 μM, respectively.

energy input: $\eta \equiv -f\hat{v}/(r\Delta\mu)$ [2]. By definition, η vanishes at $f = 0$ and at the stalling force $f_{\rm st}$. Therefore, it has a local maximum $\eta_m(\Delta\mu)$ for some $f_m(\Delta\mu)$ between $f_{\rm st} < f_m < 0$ [see Fig. 3(b) inset]. Near equilibrium, $\eta_m(\Delta\mu)$ has a constant value, $\eta_m^{\rm eq}$, along a straight line $f_m(\Delta\mu) \propto \Delta\mu$ inside Region A [2]. Far from equilibrium, we find that η_m has an absolute maximum at some $\Delta\mu > 1$, and η_m is substantially larger than $\eta_m^{\rm eq}$ as shown in Fig. 3(b). Hence, a motor achieves a higher efficiency in the far-from-equilibrium regimes [3].

Finally, to discuss the relevance of our framework to kinesin, we carried out a global fit of kinesin velocity data of Ref. [8] to our model at different external forces and two curves of force vs velocity at different ATP concentrations (see Fig. 4). Assuming that $e^{\Delta\mu} = k_0[\mathrm{ATP}]$, we obtain the best-fit values for the parameters: $\epsilon = 10.81$, $k_0 = 1.4 \times 10^5\ \mu\mathrm{M}^{-1}$, $\alpha = 0.57\ \mathrm{s}^{-1}$, $\alpha' = 1.3 \times 10^{-6}\ \mathrm{s}^{-1}$, $\omega = 3.5\ \mathrm{s}^{-1}$, $\omega' = 108.15\ \mathrm{s}^{-1}$, $\theta_a^+ = 0.25$, $\theta_a^- = 1.83$, $\theta_b^+ = 0.08$, and $\theta_b^- = -0.16$. These values are reasonable within the accepted biophysical picture of kinesin [1]. First, ϵ and k_0^{-1} represent the typical binding energy ($\sim 10 k_B T$) of kinesin with microtubules and the ATP concentration at equilibrium ($\sim 10^{-5}\mu$M), respectively. Secondly, $\theta_a^- = 1.83$ indicates that the back-steps (transitions $a \to b$) of kinesin contain most of the displacement sensitivity [1]. Moreover, our framework allows us to estimate a maximum stalling force of -7 pN, and more importantly, a run length of $\ell \simeq 0.97(2d)$ and a global ATP consumption rate of $r \simeq 111\ \mathrm{s}^{-1}$, all in excellent agreement with known values [1]. Using the above parameters, we constructed the diagram of operation for kinesin (Fig. 2), we made predictions about $\Delta\lambda$ and T_{ij} [Fig. 3(a)], and we obtained the efficiency for kinesin [Fig. 3(b)]. In particular, we find that $T_{11} \sim 10T$, the maximum value of $\Delta\lambda \sim 45\ \mathrm{pN}^{-1}\,\mathrm{s}^{-1}$, and $\Delta\lambda \sim -10\ \mathrm{pN}^{-1}\,\mathrm{s}^{-1}$ at large $\Delta\mu$. Under typical physiological conditions ($\Delta\tilde{\mu} \sim 10$–$25 k_B T$), kinesin operates at an efficiency in the range of 40–60%, also in agreement with experiments [1]. Lastly, we point out a remarkable feature: the absolute maximum of η_m occurs approximately at a $\Delta\mu$ at which $\Delta\lambda$ is also a maximum, corresponding to an energy scale of 15–$20 k_B T$ (see Fig. 3). It is interesting to note that kinesins operate most efficiently in an energy scale corresponding to the energy available from ATP hydrolysis.

In conclusion, FT links a set of physical quantities that reveal the mechanochemical couplings of a motor, and our results support a growing consensus that FT provides a possible organizing principle for driven active systems.

We acknowledge important discussions with A. Ajdari, Y. Hatwalne, J. F. Joanny, F. Jülicher, T. C. Lubensky, and J. Prost. We acknowledge support from the ESPCI (for A. W. C. L.) and from a CEFIPRA grant (for D. L.).

[1] J. Howard, *Mechanics of Motor Proteins and the Cytoskeleton* (Sinauer Associates, Sunderland, MA, 2001).
[2] F. Jülicher *et al.*, Rev. Mod. Phys. **69**, 1269 (1997).
[3] A. Parmeggiani *et al.*, Phys. Rev. E **60**, 2127 (1999).
[4] M. E. Fisher and A. Kolomeisky, Proc. Natl. Acad. Sci. U.S.A. **96**, 6597 (1999); **98**, 7748 (2001).
[5] Y. Kafri *et al.*, Biophys. J. **86**, 3373 (2004).
[6] R. Lipowsky, Phys. Rev. Lett. **85**, 4401 (2000); G. Lattanzi and A. Maritan, Phys. Rev. Lett. **86**, 1134 (2001).
[7] C. L. Asbury, Curr. Opin. Cell Biol. **17**, 89 (2005).
[8] M. J. Schnitzer and S. M. Block, Nature (London) **388**, 386 (1997); K. Visscher *et al.*, Nature (London) **400**, 184 (1999).
[9] C. M. Coppin *et al.*, Proc. Natl. Acad. Sci. U.S.A. **94**, 8539 (1997); M. Nishiyama *et al.*, Nat. Cell Biol. **4**, 790 (2002); C. L. Asbury *et al.*, Science **302**, 2130 (2003); N. J. Carter and R. A. Cross, Nature (London) **435**, 308 (2005).
[10] J. W. Shaevitz *et al.*, Biophys. J. **89**, 2277 (2005).
[11] G. Gallavotti and E. G. D. Cohen, Phys. Rev. Lett. **74**, 2694 (1995); J. Kurchan, J. Phys. A **31**, 3719 (1998); C. Maes, J. Stat. Phys. **95**, 367 (1999); D. J. Evans and D. J. Searles, Adv. Phys. **51**, 1529 (2002).
[12] G. Gallavotti, Phys. Rev. Lett. **77**, 4334 (1996).
[13] J. L. Lebowitz and H. Spohn, J. Stat. Phys. **95**, 333 (1999).
[14] J. Liphardt *et al.*, Science **296**, 1832 (2002); D. Collin *et al.*, Nature (London) **437**, 231 (2005); V. Blickle *et al.*, Phys. Rev. Lett. **96**, 070603 (2006).
[15] H. Qian, J. Phys. Condens. Matter **17**, S3783 (2005).
[16] U. Seifert, Europhys. Lett. **70**, 36 (2005).
[17] D. Andrieux and P. Gaspard, Phys. Rev. E **74**, 011906 (2006).
[18] Note that $\partial_{z_i}\partial_{z_j}\ldots\vartheta[x, y] \equiv \partial_{z_i}\partial_{z_j}\ldots\vartheta[z_1, z_2]|_{z_1=x, z_2=y}$.
[19] H. Sakaguchi, J. Phys. Soc. Jpn. **75**, 063001 (2006).
[20] K. Sekimoto, J. Phys. Soc. Jpn. **66**, 1234 (1997).